

MULTI-ENSEMBLE PROJECTION OF FUTURE COASTAL CLIMATE CHANGE

Nobuhito Mori¹, Tomoya Shimura², Sota Nakajo³, Tomohiro Yasuda¹ and Hajime Mase¹

The comprehensive understanding of future global coastal and ocean climate change due to green house effects will be required for impact assessment, mitigation and adaptation strategies of beach morphology, breakwater design in coastal and ocean engineering fields. This study analyzes future change of averaged coastal physics such as sea level rises, sea surface winds and ocean wave heights based on the climate data set combining IPCC(2007) results and the latest MRI high-resolution AGCM results. The ocean wave height is statistically projected using an empirical formula with sea surface wind by multi-model ensemble. The ensemble means and their standard deviations of coastal forces are presented for the year 2000 to 2100. The signal of future change of H_s has striped pattern in latitudinal direction and is clearer in the Southern Hemisphere than the Northern Hemisphere. The ratio of future change of H_s to the present climate is $\pm 15\%$ maximumly which is significant change than sea surface pressure and U_{10} . The large uncertainty of projected H_s can be observed around the Equator area and the Antarctic Ocean. It is found that the synoptic scale of atmospheric pressure distribution is important to estimate and to understand for the future change of SST, U_{10} and H_s .

Keywords: sea level rise, ocean wave, climate change, statistical projection, CMIP3

INTRODUCTION

Research on global climate change due to enhanced greenhouse effects on the earth's environment is changing our understanding of these phenomena to allow for assessment, mitigation and adaptation strategies for the future development of human society. From the year 1870 to 2004, the sea-level has risen at a rate of $1.7 \text{ mm} \pm 0.3 \text{ mm/yr}$, with a significant increase in the rate during the last ten years (Church and White, 2006; Church et al., 2011). The major source of sea-level rise is thermal expansion of sea water due to an increase in temperature of ocean upper layer, thus sea-level rise is a static, or long-term, side issue of climate change influencing coastal and upper ocean regions. Sea-level rise greatly impacts human activity near the coastal zone IPCC Fourth Assessment Report (IPCC-AR4, 2007) and simply exacerbates the vulnerability of coastal regions to other physical processes, such as storm surges and storm waves. Another direct consequence of sea-level rise is inundation of low-lying coastal areas, which is a long-term concern and it has been discussed wide variety fields (e.g. IPCC, 2007).

On the other hand, future changes in storm surge and ocean wave climates are a dynamic side issue of how climate change influences coastal regions (e.g. Mori et al., 2010). If extreme weather events become stronger in the future, it is necessary to seriously consider the effects of these dynamic phenomena to prevent and reduce the impact of coastal disasters. For example, the North Atlantic observed wave data shows 5 cm/yr increase of annual maxima for the last 40 years (Wang and Swail, 2002). The wave hindcasts in the Atlantic Ocean show more significant wave height increase in the region off the Canadian coast and the northwest of Ireland but less significant change in the North Sea and in the region off the Scandinavian coast (Wang and Swail, 2002). It is also reported that the significant positive long-term trends in extreme wave height near the Western coast of the US (Menéndez et al., 2008) In addition, understanding long-term changes to storm surge and storm waves are important considerations for structures near the coastal zone. For example, a coastal breakwater is designed with a maximum storm surge level and dynamic pressure from a maximum wave condition for a predetermined design lifetime. Suh et al. (2012) examined impact of climate change on a caisson type breakwater considering sea level rise, extreme wave height change and storm surge change until the end of this century. They concluded that the caisson breakwater to be designed using the projected wave height and water level in 30 years from construction. However such case study is very sensitive to assumed future change of design forces and the uncertainty of design forces should be included as an impact assessment.

Coastal erosion is another critical issue, where more than 70% of sandy beaches around the world are presently erosional. Equilibrium condition of coastal beach profile depends on seasonal or annual wave height, period and direction. The projection of future change on coastal erosion is insufficient due to information deficiencies on changes in waves and coastal currents. Therefore, future ocean wave climate change will have significant impacts on extreme and daily coastal environments. However, impact assessment of coastal erosion has strong locality and the value of global projection cannot apply to specific area or beach,

¹Disaster Prevention Research Institute, Kyoto University, Gokasho, Uji, Kyoto 611-0011, JAPAN.

²Graduate School of Engineering, Kyoto University, Kyoto daigaku-Katsura, Nishikyo-ku, Kyoto 615-8530, JAPAN.

³Department of Civil and Environmental Engineering, Kumamoto University, Kumamoto 860-8555, JAPAN.

directly. The uncertainty of future change and locality should be considered but there is few general discussion and database for regional change of coastal physics such as sea level rises, wave heights and extreme sea levels (denotes coastal physics hereafter for simplicity) from present to future. Therefore, it is important to know the fundamental characteristics of future change of coastal physics for engineering applications. However, characteristics of spatial and temporal changes of coastal physics depend on projection methods, GCMs and scenarios and are complicated and difficult to understand.

Although, it is importance of extreme climate changes of coastal physics, the averaged values are also important to understand long-term changes of coastal environment. There are several approaches to estimate these trends and variability. For example, the extreme waves and storm surges due to tropical cyclone and extra-tropical cyclone are low frequency events. Therefore, it is difficult to project their future change by the direct method (dynamic model; e.g. Mori et al., 2010; Hemer et al., 2012). A statistical approach is necessary to increase number of sample and it gives the return value of extreme sea states (e.g. Caires et al., 2006; Wang and Swail, 2006; Mori, 2012). On the other hand, a relatively large scale phenomenon such as sea level rise can be estimated by GCMs results, directly. However, even if we use the GCM results directly, there are two different types of uncertainty. First is scenario dependence uncertainty and another is performance of GCM itself. For example, IPCC-AR4 (2007) summarized about future change of atmospheric pressure that the dependence of scenario is relatively major in short-term period (less than 30 years) but it becomes minor and the model differences becomes major role for medium to long-term projections.

This paper deals with the long-term change of sea level rise and mean ocean wave characteristics based on the multi-model statistical projection using CMIP3 data set (Phase 3 of the Coupled Model Intercomparison Project) on a global scale. First, future changes of sea surface temperature and sea level rise are discussed based on the CMIP3 model ensemble. Second, the future change of sea surface wind and waves are considered based on the results of statistical projection method. Finally, general characteristics of future change of coastal physics are discussed both spatial patterns and uncertainties considering emission scenario influences.

METHODOLOGY

Ensemble projections of Sea Surface Temperature (SST), Sea Level Rise (SLR), Sea Level Pressure (SLP) and sea surface wind (U_{10}) were statistically analyzed based on CMIP3 results which were used for IPCC-AR4 (2007). In addition, the latest Japanese high resolution atmospheric GCMs (AGCM; denote MRI-AGCM3.1S and 3.2S) results were included for the analysis. The MRI-AGCM-3.1S and 3.2S were simulated with 20 km resolution under the Special Report on Emissions Scenarios (SRES) A1B for the IPCC Fifth Assessment Report (AR5) (Kitoh et al., 2009). All CMIP3 results were used for the future projection for the year 2000–2100, although the MRI models were conducted as time-slice experiments which computed 25 years as present climate (1979–2003) and future climate (2075–2099), respectively. The archived CMIP3 data by Program for Climate Model Diagnosis and Intercomparison (PCMDI, PCMDI, 2007) is 25 GCMs for A1B, A2 and B1 scenarios in the future climate. Including two MRI-AGCM GCMs, total 27 GCMs were considered for analysis. Some CMIP3 GCM results contain several different initial realizations, the mean value of each GCM was used for simplicity. The detail of GCMs and SRES scenarios are describe in Meehl et al. (2007); PCMDI (2007). The spatial resolution of CMIP3 GCMs are ranged from 100 km to 500 km, approximately and the spatial resolution of MRI-AGCM-3.1S and 3.2 is 20 km. Therefore, the different grid values were linearly interpolated into 100 km resolution for the analysis. The analysis was conducted on a global scale but the regional scale analysis in the East Asia ranged 130E–140E in longitude and 24N–40N in latitude as an example of regional behavior.

The CMIP3 data has been widely analyzed in climatology study It is found that the accuracy of pressure distribution for the present climate is quite reasonable by the multi-model ensemble mean (IPCC, 2007). On the other hand, variations of westerly wind and blockings of polar wind are not well simulated at middle to higher latitude. The El Niño-Southern Oscillation (ENSO) is also not well simulated by the CMIP3 GCMs. Therefore, we basically consider the medium to long-term trends until the year 2100 applying 36 months moving average eliminating a few years natural oscillations. The long-term trends is extracted assuming a quadric function for time history of variable at each grid point. Finally, the multi-model ensemble means and their standard deviations (uncertainty) are discussed for three different SRES scenarios. In addition, the

mean values of future change will be discussed for the year 2000 to 2100, respectively. Following above mentioned method, the coastal physics are analyzed following methods depends on the variables.

SST , SLP and U_{10} The long-term change of SST, SLR and U_{10} were analyzed above mentioned method for each SRES scenario. The differences of GCMs were also analyzed. This procedure is equivalent to IPCC-AR4. However, we focus on coastal related surface variables and their relations in this manuscript.

As similar to IPCC-AR4 and the other previous study (e.g. Gregory et al., 2001), the future change of SLR was analyzed based on CMIP3 but the rigid-lid models were excluded for the analysis. Therefore, the coupled atmospheric-ocean GCMs (AOGCM) were only took into account for the analysis. As a result, the number of model ensemble is 4-6 models, depend on the scenario, for the analysis of SLR. In addition, the barometer effect of sea level pressure was considered but it was relatively minor as discussed later ($\pm 1 \text{ ha} \simeq \text{a few centimeters}$).

Ocean wave height One of remarks of this manuscript is statistical projection of future mean wave height, monthly or annual mean fields, considering different GCMs. Wang and Swail (2006) estimated extreme wave height change from the SLP. However, we used U_{10} as predictor variable for the statistical projection. This is because a wind speed has direct relation with a wave height, if we could neglect a fetch as follows.

For example, we assume the Pierson-Moskowitz (PM) spectrum for wave field,

$$S(\omega) = \alpha_{PM} g^2 \omega^{-5} \exp\left[-\beta_{PM} \left(\frac{\omega_p}{\omega}\right)^4\right] \quad (1)$$

where S the spectrum density, ω the angular frequency, ω_p the peak angular frequency, g the gravity acceleration, $\alpha_{PM} = 8.1 \times 10^{-3}$ and $\beta_{PM} = 0.74$ the constants, respectively. The peak angular frequency of PM spectrum can be approximated by

$$\omega_p = \frac{0.855g}{U_{10}} \quad (2)$$

and using the relation of $H_s = 4\eta_{rms}$, it gives

$$H_s \simeq \frac{0.286 U_{10}^2}{g} = 0.0292 U_{10}^2. \quad (3)$$

If we follows the Wilson formula, the wave height can be approximated as $H_s^{x \rightarrow \infty} \simeq 0.0306 U_{10}^2$ for infinite fetch. The well known spectra and formula have the relation of $H_s \propto U_{10}^2$ for infinite fetch and the coefficients between H_s and U_{10}^2 are 0.02–0.03. Obviously, this relation is neglected the fetch and therefore the error will be large for developing wave field. However, this simple relation is useful for the application of long-term projections with large number of GCM ensemble and different scenarios.

Next we estimated appropriate coefficient for $H_s \propto U_{10}^2$ relation using the least square method based on ERA-40 data set (Uppala et al., 2005; ERA-40, 2005). The resolution of ERA-40 is TL159 for spectral fields and N80 quasi-regular Gaussian grid and 6 hours interval. The ERA-40 has the same resolution to CMIP3 data set. The multiple linear regression analysis for H_s was additionally conducted including SLP and gradient of SLP to improve the statistical estimation method. The obtained main empirical formula is

$$H_s[m] = 0.0264 \times U_{10}^2[m/s] + 1.03 \quad (4)$$

where 0.0264 [s^2/m] is tuning coefficient and 1.03 in meter is bias which corresponds to swell height without wind condition. Figure 1 shows relationship between H_s and U_{10} with ERA-40 data. The absolute error and RMS error by Eq.(4) is 0.25 m and 0.33 m, respectively. The accuracy of Eq.(4) is relatively poor in lower wind speed region because of infinite fetch assumption. The infinite fetch assumption has two major errors. One is error due to developing sea states and another error is swell effects. Therefore, it is expected that the relation of Eq.(4) may work at the middle to higher latitudes where wind sea is relatively dominant, but it may not work well at lower latitude.

Alternative statistical approach is use of other predictor or multiple regression analysis. There is no big differences use of other predictors such as SLP and δSLP for H_s estimation. For example, the absolute error

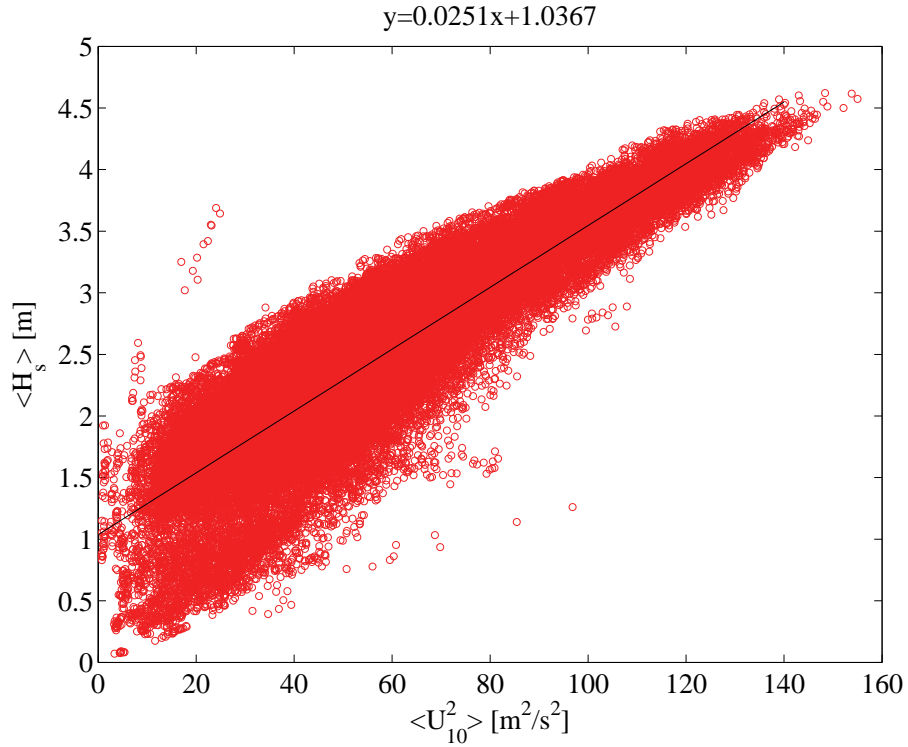


Figure 1: Estimation of H_s by U_{10}^2

and RMS error by the multiple regression model of U_{10}^2 and δSLP , become 0.26 m and 0.33 m, respectively. As shown in Figure 1, the bias and error mainly exist around lower value of H_s and the dynamic wave model is required for reduced error of estimation, obviously. It is limitation of using this kind of simple statistical model.

The future change of coastal physics base on the above summarized methods will be discussed next section. The annual changes and trends will be discussed for the year 2000 to 2100.

RESULTS AND DISCUSSION

The multi-model ensemble and multi scenario ensemble were conducted using statistical projection based on CMIP3 model. The results of analysis show that the different scenario changes the magnitude of signal, future change, but the projected spatial patterns are quite similar. Therefore, the results of SRES scenario A1B will be mainly discussed in this section. The results of different scenarios will be summarized at the end of this section.

Future change of SST, SLP and SLR

Figure 2 shows spatial distribution of mean SST change, ΔSST , for the year 2000 to 2100 by CMIP3 ensemble for SRES scenario A1B. Although the analysis method is slightly different, the spatial pattern of ΔSST is quite similar to IPCC-AR4 (2007). The signal of future change is positive on a global scale and the magnitude of ΔSST about 0.2-0.3 degree is expected from the Equator to lower latitude region. The local SST change can be observed around the North West Pacific Ocean, and the South Indian and the Atlantic Ocean at the Southern Hemisphere. These are mainly due to future changes of the Kuroshio current, the South Indian current and the South Atlantic current. The model differences are quite significant around these currents (not shown in figure) and therefore the uncertainly of projection around these regions is larger than other areas.

The SLR is important issue of impact assessment of climate change for coastal region. As similar

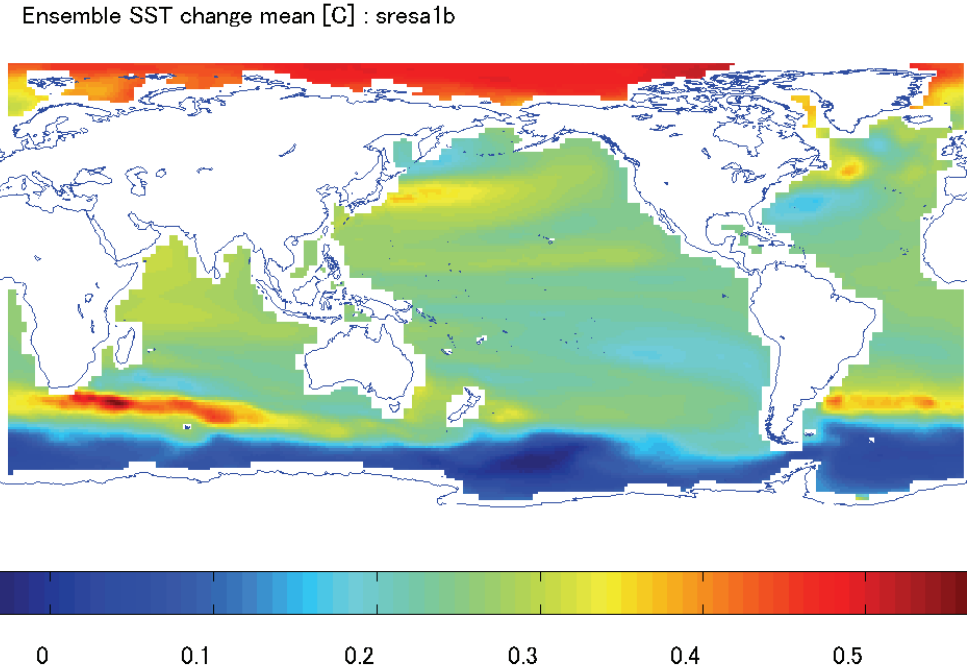


Figure 2: Future change of SST at year 2100 (SRES A1B)

to SST shown in Figure 2, Figure 3 shows spatial distribution of mean SLR for the year 2000 to 2100 by CMIP3 ensemble with SRES scenario A1B. The rigid-lid models were excluded from the analysis. Therefore the projection of SLR is slightly different from IPCC-AR4 (2007) but these are quite similar. The signal of SLR at the year 2100 has both positive and negative (sea level down) as similar to CMIP3 results and the spatial pattern of SLR is more inhomogeneous than that of SST. The negative sea level change is expected around the Antarctic Ocean and the North West Atlantic near US coast. On the contrary, the significant increase of SLR is expected around the Kuroshio current, the South Indian current and the South Atlantic current regions. The general pattern of SLR is quite similar to future SST change as shown in Figure 2. This is due to contribution of thermal expansion of water column to SLR. The ice melting is another factor to be considered but we would not discussed in detail. Additional factor to change the sea level is barometer effects. If the barometer effect can be regarded as 1 ha = 1 cm, the future change of SLP due to barometer effects is 3 cm maximumly. This effect is included in the previous analysis of SLR.

Figure 4 shows time history of spatial averaged SLR from the year 2000 to 2100 both the global scale and the East Asia. The future change of SLR is 0.27 m on a global scale and is slightly small in the East Asia. There is no big difference between the global scale and the East Asia scale but the standard deviation of the East Asia scale is much larger than that of global scale. The uncertainty of model projection becomes significant in the regional scale and it should be considered carefully for an impact assessment.

Surface Wind and Ocean Wave

The spatial distribution of ΔU_{10} basically corresponds to gradient of δSLP . There are decreasing regions of ΔU_{10} in the middle latitude both Hemispheres and the around Equator region. The increasing ΔU_{10} regions are offshore of Peru and off Antarctic Ocean. The decreasing ΔU_{10} on the Equator region indicates weaker trade wind in the future climate and it is related with the SST and ENSO projection as briefly discussed in the previous section. The annual mean wind speed is lowest around the Equator and is increased as latitude becomes higher. The ratio of future change to the present climate is $\pm 5\%$ maximumly which

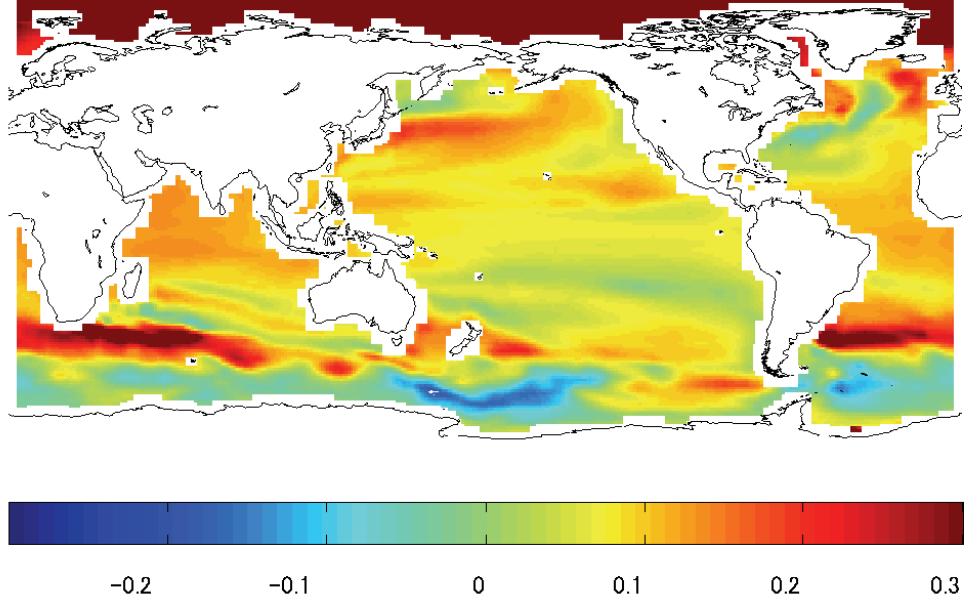


Figure 3: Projected SLR at year 2100 (SRES A1B)

becomes remarkable around the Equator. The uncertainty of projection will be discussed with the projection of H_s because it is parameterized by the U_{10}^2 .

Figure 5 shows spatial distribution of future change of mean wave height, ΔH_s , based on Eq.(4), for the year 2000 to 2100 by CMIP3 ensemble with SRES scenario A1B. There is clear latitudinal dependence of ΔH_s , stripe pattern in the latitudinal direction, which was pointed out by dynamic wave projection Mori et al. (2010). The statistical projection has stronger latitudinal stripe pattern than the dynamic wave projection. This is due to neglection of wave dispersion and swell in the statistical projection. There are both positive and negative regions of ΔH_s . The signal of change is clear in the Southern Hemisphere. The ratio of future change of H_s to the present climate is $\pm 15\%$ maximumly which is remarkably larger than ΔU_{10} . The uncertainty of projection can be observed around the Equator area and the Antarctic Ocean. The model standard deviations have similar magnitude to model ensemble mean in these areas. The future change of H_s on the Equator is related with trade wind change (ENSO) and the future change around the Antarctic Ocean is related with polar ward shift of pressure system. Therefore, the regional impacts of future mean H_s change are influenced by different large scale climate system changes (i.e. teleconnection).

Figure 6 shows time history of spatial averaged ΔH_s from the year 2000 to 2100 both the global scale and the East Asia. The spatial averaged ΔH_s shows about +2 cm change on a global scale which corresponds 0.5-1 % change in the ratio to annual mean value. The spatial distribution of ΔH_s has both positive and negative changes as shown in Figure 5, although the signal of future change is cancelled out on a global scale. The future trend of ΔH_s is slightly negative in the East Asia and the model standard deviation is a few times larger than mean value. The projected ΔH_s in the East Asia is varied from +3 cm to -9cm with the range of $\pm \sigma$, it corresponds to 5-6 % change respect to the present climate. The uncertainty of ΔH_s is quite large and it is largest future change ratios between SST, SLR and SLP.

General Discussions and Influence of Emission Scenario

The future projection of SST, SLR, SLP, U_{10} and H_s of SRES scenario A1B has been discussed to understand spatial and temporal changes at the year 2000 to 2100. The influence of emission scenario was

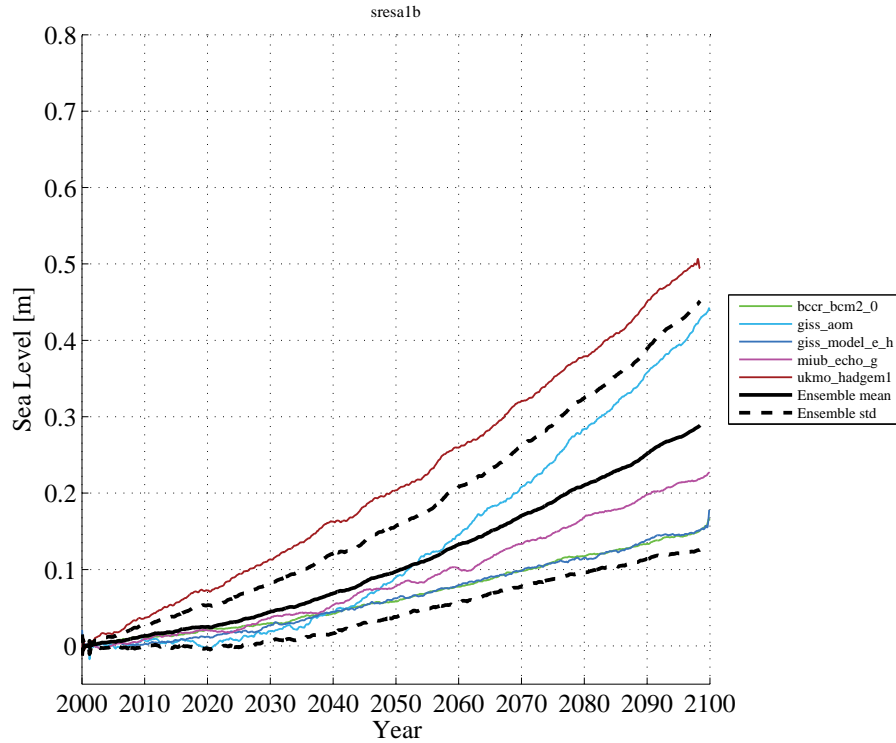


Figure 4: Annual change of SLR for year 2000 to 2100: SRES A1B (thin lines: individual GCMs, thick solid line: ensemble mean, thick dashed line: standard deviation)

examined for SRES A2 and B1 scenarios. There is little influence of scenario differences on the spatial pattern of future change, although the magnitudes are different. The largest change is expected by the SRES scenario A2, smallest one is the SRES scenario B1 and the SRES scenario A1B is the middle of three scenarios. For example, the projected SLRs at the year 2100 are 1.86 m and 0.87 m by SRES A2 and B1 scenarios on a global scale, respectively. The difference of projected SLR is more than two times depends on the choice of scenario. The standard deviation between models is basically larger as mean value larger. The signal of future change in the East Asia region is relatively significant than the global mean because it located middle latitude. Similar local characteristics can be seen in the other regions depend on the phenomena. Both model uncertainty, scenario influence and local variability should be carefully considered for impact assessment such as beach morphology assessment.

As discussed in previous section, the future change of individual phenomenon have different spatial distribution and uncertainty. However some phenomena has correlation each other. For example, SST and SLR is highly related with correlation coefficient of 0.9. The gradient of SLP is also very weakly correlated with SST (correlation coefficient of 0.3). Obviously H_s and U_{10} is related but gradient of SLP has the significant correlation coefficient of 0.6. Therefore, the synoptic scale of atmospheric pressure distribution is important for future change of SST, U_{10} and H_s . It is important to understand the local impact of teleconnection between synoptic change to wave climate.

CONCLUSIONS

This paper discussed the long-term change of sea surface temperature, sea level rise and mean wave characteristics based on the statistical projection using CMIP3 and the latest MRI high resolution GCM results.

Both global scale and regional scale changes were discussed and the East Asia was selected one of example of local behavior of future climate projection. The projected mean future change of SLR is 0.27

m on a global scale and is slightly small in the East Asia. The uncertainty of model projection for SLR becomes large in the regional scale and it should be considered carefully for an impact assessment.

The statistical projections of U_{10} and H_s have striped pattern in the latitudinal direction. The large uncertainty of projection H_s can be observed around the Equator area and the Antarctic Ocean. The future change of H_s on the Equator is related with trade wind change (ENSO) and the change around the Antarctic Ocean is related with polar ward shift of pressure system. Therefore, the synoptic scale of atmospheric pressure distribution is important to estimate and to understand for future change of SST, U_{10} and H_s for coastal and ocean engineering applications.

ACKNOWLEDGEMENT

The authors acknowledge the developers of the CGCMs used in this study and World Climate Research Programme's CMIP3 project. This research was supported by the SOSEI Program and the Kakenhi Grant-in-Aid of the Ministry of Education, Culture, Sports, Science, and Technology (MEXT).

References

- Caires, S., V. Swail, and X. Wang. 2006. Projection and analysis of extreme wave climate, *Journal of climate*, 19(21), 5581–5605.
- Church, J. and N. White. 2006. A 20th century acceleration in global sea-level rise, *Geophysical Research Letters*, 33(1), L01602.
- Church, J., N. White, L. Konikow, C. Domingues, J. Cogley, E. Rignot, J. Gregory, M. van den Broeke, A. Monaghan, and I. Velicogna. 2011. Revisiting the earth's sea-level and energy budgets from 1961 to 2008, *Geophysical Research Letters*, 38(18), L18601.
- ERA-40. 2005. ECMWF 40 Year Re-analysis.
- Gregory, J., J. Church, G. Boer, K. Dixon, G. Flato, D. Jackett, J. Lowe, S. O'Farrell, E. Roeckner, G. Russell, et al.. 2001. Comparison of results from several aogcms for global and regional sea-level change 1900–2100, *Climate Dynamics*, 18(3), 225–240.
- Hemer, M., K. McInnes, and R. Ranasinghe. 2012. Climate and variability bias adjustment of climate model-derived winds for a southeast australian dynamical wave model, *Ocean Dynamics*, 1–18.
- IPCC. 2007. IPCC fourth assessment report (AR4). <http://www.ipcc.ch/>.
- Kitoh, A., T. Ose, K. Kurihara, S. Kusunoki, M. Sugi, and KAKUSHIN Team-3 Modeling Group. 2009. Projection of changes in future weather extremes using super-high-resolution global and regional atmospheric models in the KAKUSHIN Program: Results of preliminary experiments, *Hydrological Research Letters*, 3, 49–53.
- Meehl, G., C. Covey, T. Delworth, M. Latif, B. McAvaney, J. Mitchell, R. Stouffer, and K. Taylor. 2007. The WCRP CMIP3 multi-model dataset: A new era in climate change research, *Bulletin of the American Meteorological Society*, 88, 1383–1394.
- Menéndez, M., F. Méndez, I. Losada, and N. Graham. 2008. Variability of extreme wave heights in the northeast Pacific Ocean based on buoy measurements, *Geophysical Research Letters*, 35(22), L22607.
- Mori, N.. 2012. *Cyclones Formation, Triggers and Control*, Chapter Projection of Future Tropical Cyclone Characteristics based on Statistical Model, in press. Nova Science Publishers.
- Mori, N., T. Yasuda, H. Mase, T. Tom, and Y. Oku. 2010. Projection of Extreme Wave Climate Change under Global Warming, *Hydrological Research Letters*, 4(0), 15–19.
- PCMDI. 2007. Program for Climate Model Diagnosis and Intercomparison (PCMDI).
- Suh, K., S. Kim, N. Mori, and H. Mase. 2012. Effect of climate change on performance-based design of caisson breakwaters, *Journal of Waterway, Port, Coastal, and Ocean Engineering*, 138(3), 215–225.

- Uppala, S., P. Källberg, A. Simmons, U. Andrae, V. Bechtold, M. Fiorino, J. Gibson, J. Haseler, A. Hernandez, G. Kelly, et al.. 2005. The ERA-40 re-analysis, *Quarterly Journal of the Royal Meteorological Society*, 131(612), 2961–3012.
- Wang, X. and V. Swail. 2002. Trends of Atlantic wave extremes as simulated in a 40-yr wave hindcast using kinematically reanalyzed wind fields, *Journal of Climate*, 15(9), 1020–1035.
- Wang, X. and V. Swail. 2006. Climate change signal and uncertainty in projections of ocean wave heights, *Climate Dynamics*, 26(2), 109–126.

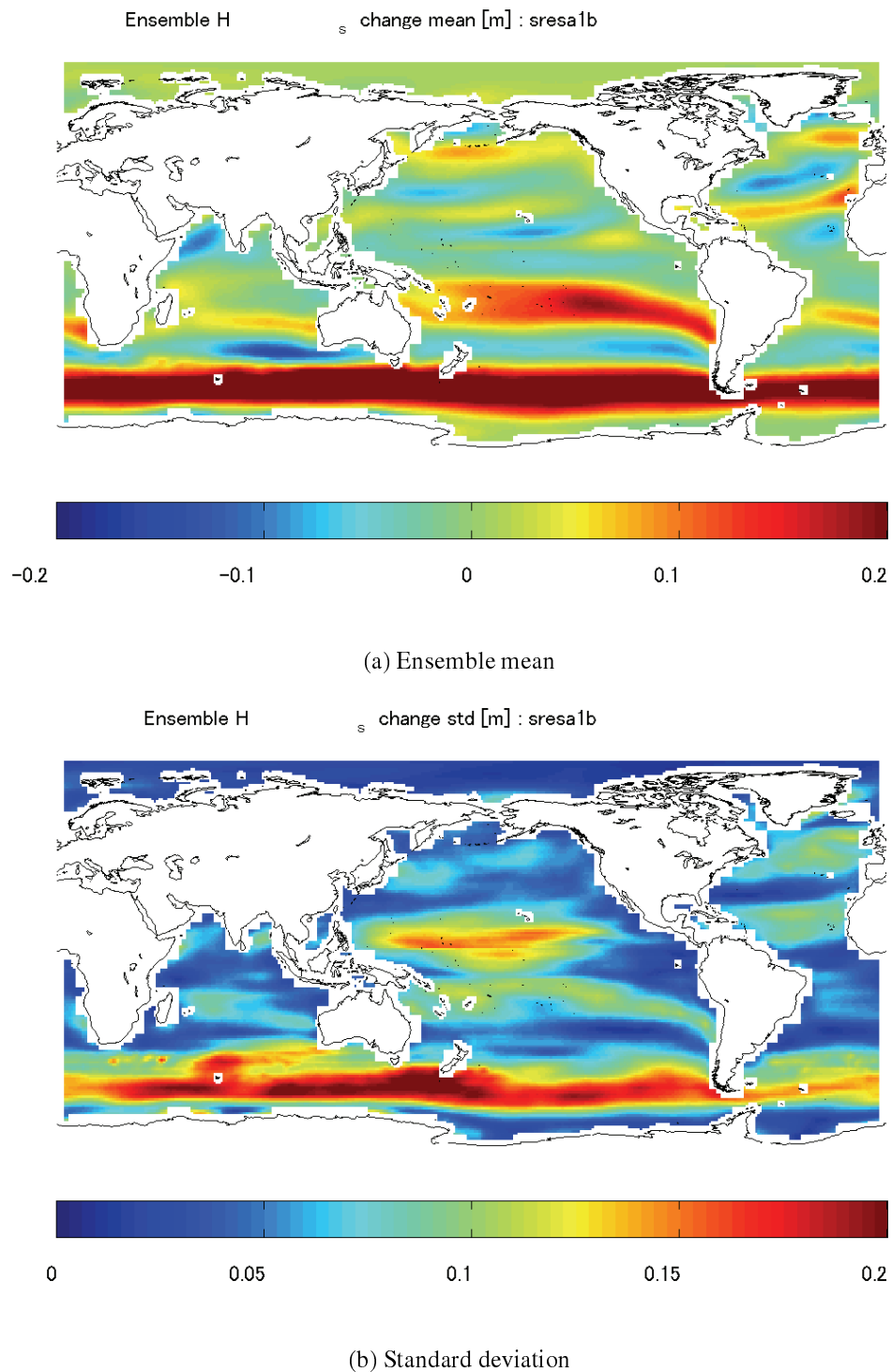


Figure 5: Future change of H_s at year 2100 (SRES A1B)

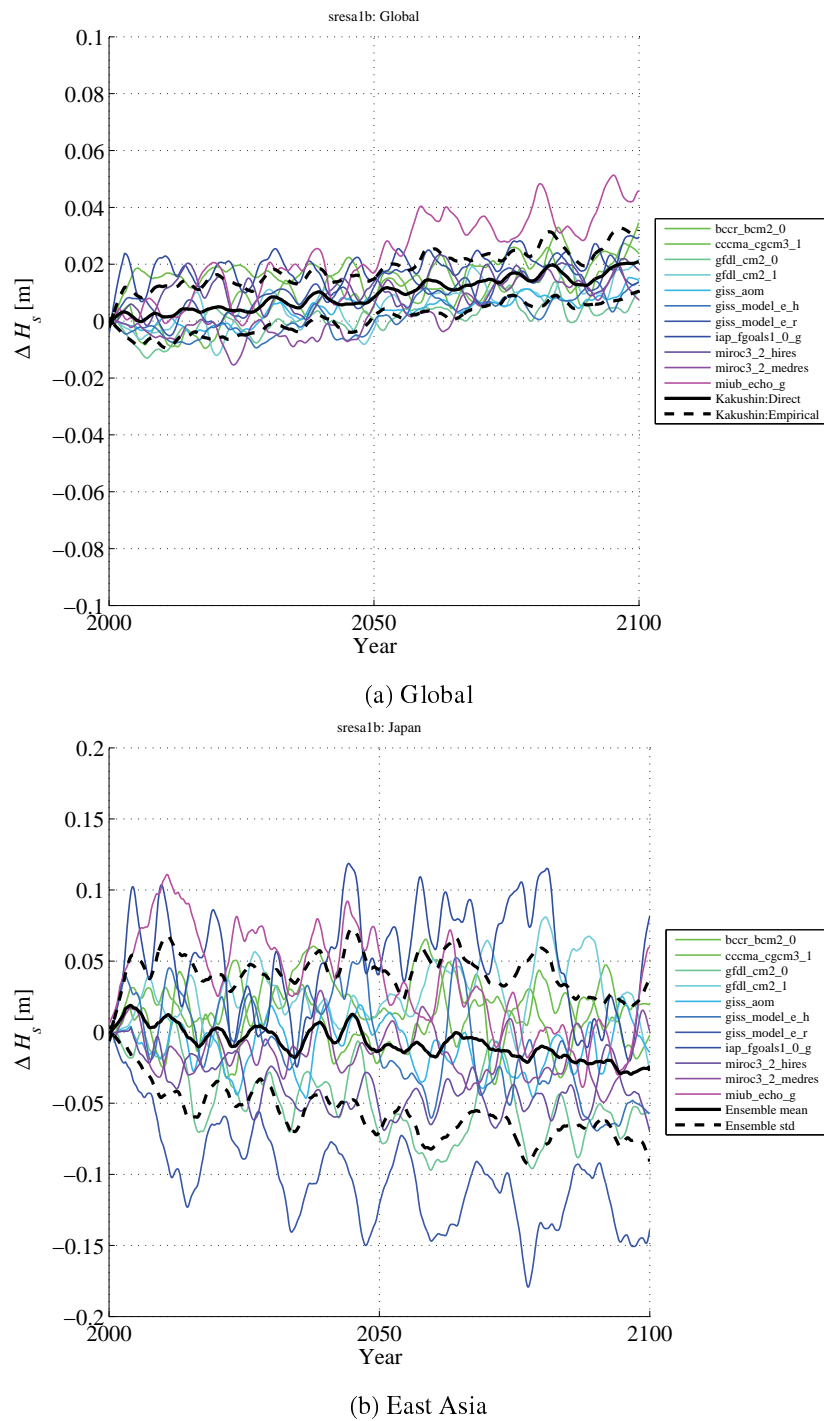


Figure 6: Annual change of H_s for year 2000 to 2100: SRES A1B (thin lines: individual GCMs, thick solid line: ensemble mean, thick dashed line: standard deviation)